Sugarcane Peel Ash as a Sorbent for Methylene Blue

Edwin A. Ofudje,^{a,*} Khairia Mohammed Al-Ahmary,^b Elham A. Alzahrani,^c Salah Ud Din,^d and Jamelah S. Al-Otaib ^e

Sugarcane peel waste (SPW) modified by combustion was used as a sorbent for methylene blue (MB) in aqueous medium under the influence of parameters such as pH of the medium, initial MB concentrations, contact time, SPW dosage, and temperature using batch experiments. The microstructure of the adsorbent was analyzed using Fourier infrared spectroscopy (FT-IR), scanning electron microscopy (SEM), energy dispersive X-ray analysis (EDX), and X-ray diffractometer (XRD). The quantity (mg/g) of adsorbed MB increased with increased contact time, rise in dye concentration, as well as the solution pH. Similarly, the temperature of the system improved the sorption effectiveness with maximum sorption capacity of 65.4 and 81.2% at 45 °C and 55 °C for USPW and MSPW, respectively. At an initial MB concentration of 100 mg/L, temperature of 45 °C and 55 °C, pH of 4, and reaction times of 80 and 60 min for unmodified sugarcane peel waste (USPW) and modified sugarcane peel waste (MSPW), respectively, optimal MB adsorption of 22.6 and 33.2 mg g⁻¹, respectively, was achieved.

DOI: 10.15376/biores.19.4.9191-9219

Keywords: Adsorbent; Ash; Cellulose; Biomass; Dye; Isotherms; Kinetics

Contact information: a: Department of Chemical Sciences, Mountain Top University, Ogun State, Nigeria; b: Department of Chemistry, College of Science, University of Jeddah, Jeddah, Saudi Arabia; c: Department of Chemistry, College of Science, University of Ha'il, 81442 Hail, Saudi Arabia; d: Department of Chemistry, University of Azad Jammu and Kashmir, Muzaffarabad, 13100, Pakistan; e:Department of Chemistry, College of Science, Princess Nourah Bint Abdulrahman University, P.O. Box 84428, Riyadh 11671, Saudi Arabia; *Corresponding author: eaofudje@mtu.edu.ng

INTRODUCTION

Water pollution can occur in various ways, and the haphazard release of manufacturing waste and effluents from municipal areas is one of the most prominent sources of poor water quality. Most water bodies in developing nations, such as Nigeria, are polluted by industrial effluents. Organic dyes are widely utilized in diverse industries, including plastics, textiles, food, paper, cosmetics, and detergents (Burtch *et al.* 2014). These industries often release their waste products into the water system without proper treatment, thus contributing to environmental challenges. The negative impacts of the continuous discharge of dyes into water systems are a serious problem for numerous governments. Some of the key issues related to dye-tainted water include non-biodegradation, toxicity, and reduced light penetration (Burtch *et al.* 2014; Chen *et al.* 2015; Zha *et al.* 2019). Even at low concentrations below 1 ppm, the release of dyes into water bodies is quite noticeable, and a few dyes can easily cause water coloring (Cui *et al.* 2019). Aquatic creatures require a source of light for energy generation. However, the coloring of the water surface hinders the penetration of light, thus generating an ecosystem imbalance (Oladoye *et al.* 2022).

Wastewater loaded with methylene blue (MB) dye released into the environment has been reported to cause health issues in humans, such as necrosis, cyanosis, vomiting, jaundice, Heinz body formation, enhanced rate of heart disease, and shock (Oladoye *et al.* 2022; Uzosike *et al.* 2022). Furthermore, it has been reported that the presence of MB in plants could lead to retarded growth, pigment reduction, and a significant impact on photosynthetic activity (Moorthy *et al.* 2021). Thus, these consequences, which are associated with the release of MB dye into the environment, necessitate the search for an effective material for MB removal from wastewater prior to its discharge.

The treatment of wastewater is often done through the use of different methods such as coagulation, ion exchange, chemical precipitation, membrane processes, solvent extraction, filtering, and sedimentation (Adeogun et al. 2012; Burtch et al. 2014; Chen et al. 2015; Ahmad et al. 2020). The major limitations of membrane technology are (i) waste particles get stuck, thus causing blockage, and as such fouling occurs in the membrane and (ii) it requires high operation and maintenance costs due to higher energy consumption (Gregorio and Eric 2018; Queen et al. 2022). Biological treatments take a long time for degradation to occur and require a well-adjusted environment for microbes to survive (Adeogun et al. 2012). Chemical treatment of wastewater often leads to the production of high sludge and toxic chemicals, and it suffers from disposal and handling challenges (Queen et al. 2022). The need for the use of several non-reusable chemicals, such as flocculants and coagulants, and the need to continuously monitor the physicochemical properties of the effluent pH are major limitations of the coagulation/flocculation method (Gregorio and Eric 2018; Queen et al. 2022). A major drawback of chemical oxidation is that it requires a long time to prepare the required chemicals, transport them, and manage the oxidants. Additionally, because some dyes are resistant to chemical oxidation, the need to produce high amounts of ozone could lead to the formation of intermediates, release of volatile compounds, and generation of sludge (Ofudje et al. 2014; Gregorio and Eric 2018;). The high cost of maintenance, cost of obtaining selective resin, and long period of time during regeneration are major drawbacks of the ion exchange method (Gregorio and Eric 2018; Queen et al. 2022). Furthermore, ion exchange requires a large volume of columns and physicochemical pretreatment, which makes this method not cost effective (Gregorio and Eric 2018; Cardenas et al. 2020).

Perhaps because of the issues just discussed, the most widely used method for dye removal from water is adsorption; it has been reported to be cost-effective, easy to operate, and highly efficient (Ofudje *et al.* 2022a; Neolaka *et al.* 2023). Some adsorbents such as kaolin (Yavuz and Saka 2013), magnetic walnut shells (Uzosike *et al.* 2022), Bali cow bones (Neolaka *et al.* 2023), cow dung, sludge biochar, and rice husk (Ahmad *et al.* 2020), bagasse-bentonite (Santhi *et al.* 2009), modified Tamazert kaolin (Boukhemkhem and Rida 2017), and Korean cabbage waste (Sewu *et al.* 2016) have been reported for their potency to reduce dyes in contaminated environments. The effectiveness of these adsorbents for removal of diverse dyes from water may be related to their complexity as well as the inclusion of lignin and cellulose components.

Because commercial activated carbon is costly and the cost increases with the quality, adsorbents produced from agricultural wastes have attracted interest because of the simplicity of porous structure development arising from carbonization or ashing. Cost is a key factor when choosing agricultural waste and modification treatments.

There have been limited studies evaluating the cost estimates for modified sugarcane bagasse adsorbents, making it challenging to assess both material and processing expenses. However, some research has shown that modified agricultural wastes offer a significant price advantage over commercial adsorbents. For instance, citric acid-modified sugarcane bagasse costs \$4.76 per kilogram, significantly less than commercial activated carbon at \$56.06 per kilogram (Gupta *et al.* 2018). Similarly, Fingolo *et al.* (2020) used techno-economic assessment of full-scale plants of pyrolyzed bagasse to show that this can be an economically-competitive alternative raw material to produce activated carbons at broad range of activation conditions that would enable this sustainable technology. This reuse not only promotes waste material utilization but also reduces waste disposal costs, which can be higher than the modification costs. Overall, the available studies suggest that modifying agricultural waste is a cost-effective method for producing bio-adsorbents for environmental remediation.

With the increase in the production of agricultural waste every year, these waste biomasses appear to be attractive materials for the production of adsorbents. They are easily accessible, inexpensive, renewable, and ecologically friendly. These agricultural waste structures have low specific surface areas, which often hinder their interactions with many pollutants (Liu et al. 2020). Therefore, it is essential to modify their structures to improve their adsorption properties for pollutants (Ding et al. 2014). It has been documented that the modification of agricultural wastes alters their physicochemical properties such as porosity, surface area, hydrophilic/hydrophobic behaviour, and functional groups, which often results in improved adsorption performance of the adsorbent (Liu et al. 2022). Sugarcane, which is widely employed in the manufacturing of sugar and alcohol, is the most prevalent lignocellulosic material among numerous agricultural crop wastes in tropical regions (Peng et al. 2009). Sugarcane is widely consumed in Nigeria, and the wastes (peels) generated are frequently left in open places, constituting environmental pollution and having minimal economic value. Ash biomass (MSPW) offers a higher surface area, better functionalization, greater stability, tends to be more resistant to biological or chemical decomposition, thus allowing it to be used multiple times. It contains less organic content (like lignin, cellulose, and hemicellulose), leaving behind a cleaner, more active adsorbent when compared with SPW. This reduces potential interference with the adsorption process, and higher adsorptive capacities, making the MSPW a more efficient and versatile adsorbent than unmodified biomass. Thus, selecting sugarcane peel waste as an adsorbent will not only eliminate it from the environment as a pollutant, but also become a value-added material in wastewater treatment.

Sugarcane peel waste was deployed as a starting material for ash production through heat treatment and used as an adsorbent for the removal of MB *via* a batch process under various variables, such as contact time, adsorbent dosage, solution pH, temperature, and concentration of MB. Scanning electron microscope (SEM), Fourier infrared spectroscopy (FT-IR), energy dispersive X-ray analysis (EDX), thermal gravimetric analysis (TGA), differential thermal analysis (DTA), and X-ray diffractometer (XRD) were used to provide detailed information on the adsorbent composition and crystallography, while isothermal, kinetic, and thermodynamic investigations were performed on the adsorption data.

EXPERIMENTAL

MB Solution Preparation and other Chemicals

Without further purification, 3,7-bis(dimethylamino)-phenothiazin-5-ion chloride (MB) (MG, 98.5% purity; Fluka) was used. In a volumetric flask, 1 g of MB was placed in 1 dm³ of distilled water to make a stock solution, that was then used to prepare several concentrations. pH adjustment was done by adding either of 0.1 M HCl (37% purity), or 0.1 M solution of NaOH (98% purity), Fluka.

Biomass Ash Preparation

Untreated sugarcane peel waste, which was the back of the stalk, was crushed, cleaned using hot water, treated with NaOH, dried at 100 °C for 12 h, and labeled as untreated sugarcane peel waste (USPW). Calcinations of USPW were performed in a muffle furnace at 800 °C for 3 h in three stages to give a physically modified form of the biomass referred to as modified sugarcane peel waste. Prior to further analysis, the sample was maintained in an airtight bag and labelled with modified sugarcane peel waste (MSPW). Figure 1 shows a schematic of the synthesis of USPW and MSPW, and the adsorption of methylene blue.

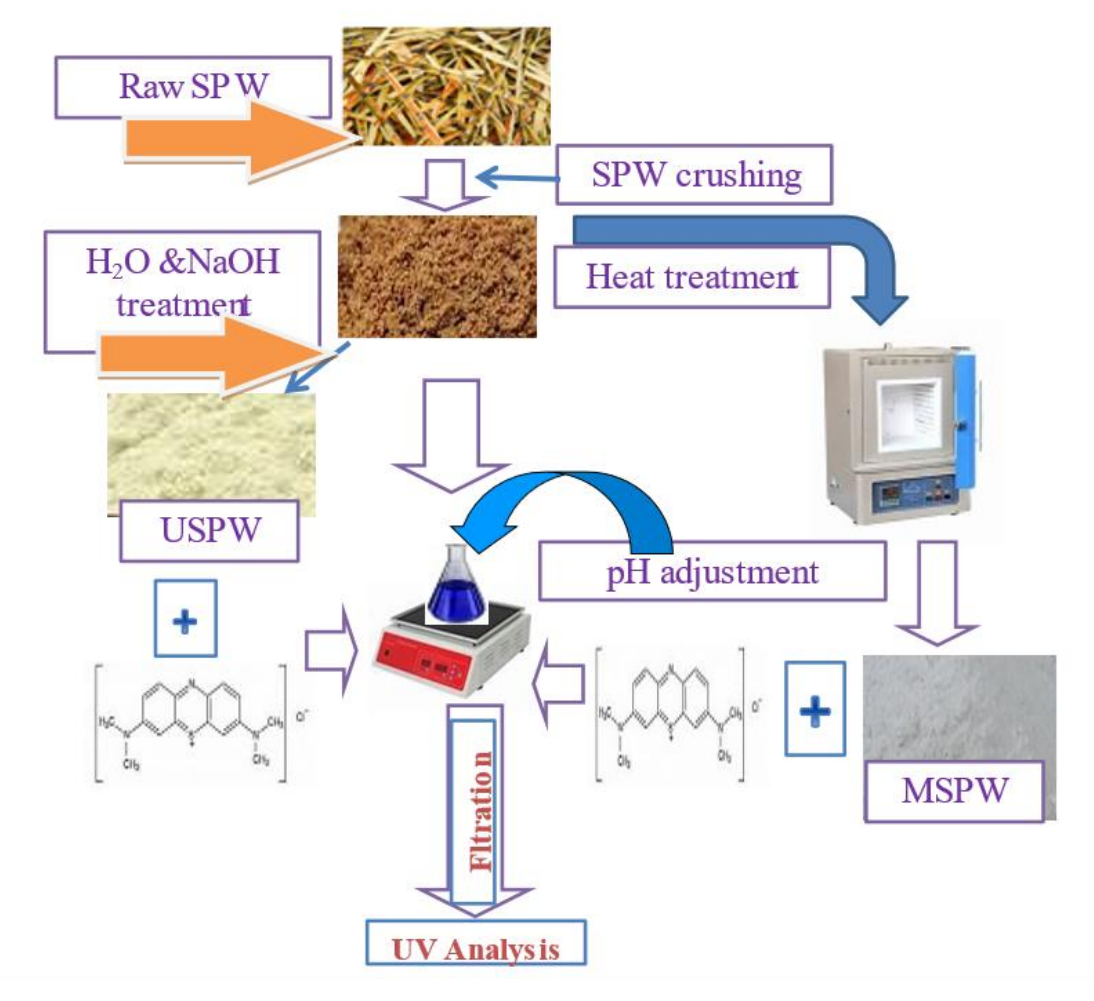


Fig. 1. Schematic for the synthesis of USPW and MSPW and adsorption of methylene blue

Characterization Technique

Distribution particle size of the adsorbent was quantified on a micrometre scale by means of a Nanotrac with Microtrac FLEX 10.5.2 (USA) system. About 0.1 g of the biomass ash sample was dispersed in 25 mL Millipore water using 100 mL beaker and sonicated for 20 mins before the analysis was performed so as to reduce the degree of agglomeration of the particles.

Imaging of the powder was obtained with a scanning electron microscope (SEM) (Hitachi, Japan S-3000H electron microscope). Samples were sputter coated with gold and placed in a sample holder. The surface morphology was then observed at an accelerating voltage of 15kV.

FT-IR transmission using the KBr technique was deployed to investigate the absorbance bands of the sugarcane bagasse (SB) and the MB. The evaluation was performed using homogenized pellets of 1:99% of KBr and the adsorbent powder and pressed at about a load of 5 tons to form pellet of 2 mm diameter. Scans were performed with a 45 scan and recorded in the wave number range of 4000 to 400 cm⁻¹ using a Shimadzu 8400S FT-IR instrument (Japan).

The X-ray Diffraction (XRD) technique was used to determine the crystallographic structure. Samples were ground into a fine powder to ensure it was homogeneous before it was placed in the sample holder. X-ray diffraction was then performed using a Miniflex II diffractometer (Rigaku, Tokyo, Japan) (Cu K = 1.5405 Å) in the range of 10 to 45°. The diffraction patterns were collected at incremental step size of 0.02 and the various peaks developed were compared with standards.

An SDT Q600 V8.3 Build 101 simultaneous DSC-TGA instrument (USA) was used to investigate the thermal behavior of the adsorbent. About 0.1 g of the sample was dispersed in 50 mL of millipore water in a 100 mL beaker and sonicated for 10 mins prior to analysis to minimize the degree of agglomeration of particle. The measurement was done beginning from room temperature to 800 °C under air flow (100 mL·min⁻¹) at a heating rate of 5 °C·m⁻¹. The Universal V4.7A TA software package was used to analyze the data. The zeta potential was measured with a Zetasizer Nano ZS instrument (Malvern, UK). Prior to measurement, about 0.15 mg of the sample were ground and dispersed in distilled water to ensure proper light scattering for zeta potential analysis. Thereafter, sonication was done for 10 mins to help break up any particle agglomerates and ensures uniform dispersion. The percentage abundance of the elemental composition was determined with A G. Vario EL analyzer (Germany). The sample was introduced into the analyzer's combustion chamber, and burned at a temperature of 900 °C. After combustion, the produced gases were separated and passed through a thermal conductivity detector (TCD). Based on the signal response from the detector, the amount of C, N, and H were quantified. For oxygen measurement, a separate pyrolysis method was used, where the sample was heated in an inert atmosphere, and the produced CO was analyzed. The measurement of the surface area, pore volume, and pore size of the adsorbent was done with the help of a Quantachrome NOVA 2200C device (USA). The adsorbent sample was first degassed under vacuum at a temperature of 100 °C to remove any contaminants such as moisture, air, etc. from the pores. In the Quantachrome NOVA 2200C analyzer, nitrogen (N2) was used as the adsorbate gas. Nitrogen molecules adsorb onto the surface of the sample and into its pores. After the adsorption, the system reduces the pressure, and the amount of nitrogen desorbed was measured.

Adsorption Studies

Twenty milligrams of sugarcane were carefully weighed into a 250 mL Erlenmeyer flask made up of 25 mL of 150 mg/L MB solution. 0.1 M HCl or NaOH solutions were used to modify the pH and were kept on an orbital shaker to equilibrate at 150 rpm. At different time intervals between 5 to 120 min and MB concentrations of 25 to 150 mg/L, samples were withdrawn, filtered, and the filtrate was tested using a UVvisible spectrophotometer. The variations of each parameter are presented in Table 1.

The removal amount of MB (mg/g), and the removal efficiency was calculated as follows,

$$R\% = \frac{c_i - c_f}{c_i} \times 100$$

$$q_e = \frac{c_i - c_f}{m} \times V$$
(2)

where C_i and C_f (mg/L) are the MB concentrations at the initial stage and at equilibrium, and m and V are the adsorbent mass (g) and the solution volume of the dye used (L). The experiments were obtained in duplicate, and the average values were determined and reported.

Table 1. Variations of the Parameters

Parameters	Variations of Parameters		
Contact time	5 to 100 mins		
Initial MB concentrations	20 to 100 mg/L		
SPW dosage	5 to 25 mg		
temperature	25 to 85 °C		
pH			

RESULTS AND DISCUSSION

Characterization

Table 2 summarizes the chemical and physical characteristics of sugarcane peel waste. The elemental compositions of USPW and MSPW as reported are C (46.2, 49.3%), O (50.2, 40.7%), H (1.3, 6.8%), and N (2.3, 3.2%). After physical alteration, the carbon percentage abundance increased, which could be a result of burning the organic matter in the biomass. USPW and MSPW had surface areas, pore volumes, and pore sizes of $(74.3, 136.6 \text{ m}^2/\text{g})$, $(0.24, 0.33 \text{ cm}^2/\text{g})$, and (3.22, 5.63 nm) respectively.

Table 2. Elemental Composition and Physical Characterization of SPW

F	Parameters	USPW	MSPW	
Zeta potential	pHzPc	3.68	5.80	
Elemental	%C	46.20	49.30	
Analysis	%O	50.20	40.70	
	%Н	1.30	6.80	
	%N	2.30	3.20	
	Pore volume (cm²/g)	0.245	0.331	
N₂ gas Adsorption Analysis	Average pore Size (nm)	3.22	5.63	
	Surface area (m²/g)	74.30	136.56	

(2)

The physical change in the biomass *via* combustion and ashing resulted in an increase of the solid's surface area per unit mass. Figure 2 shows the microstructure of the USPW, MSPW before and after MB adsorption (Fig. 2a-c). The microstructure before modification revealed a smooth surface, but after modification, the structure consisted of porous nanocrystals with holes and these holes disappeared after the adsorption of MB. The scanning electron microscopy (SEM) investigation on how methylene blue (MB) reacts with biomass ash provides detailed insights into the adsorption process and the changes that occurred on the surface morphology of the ash. After the adsorption of methylene blue, the SEM image showed significant changes on the surface of biomass ash. The MB molecules adhered to the surface and pores of the ash, covering the visible porosity of the biomass ash before adsorption thus indicating that MB has successfully entered the pores and occupied the internal spaces. The particle size investigation of the adsorbent is shown in Fig. 2d which revealed that the average particles distribution was 48.6 nm.

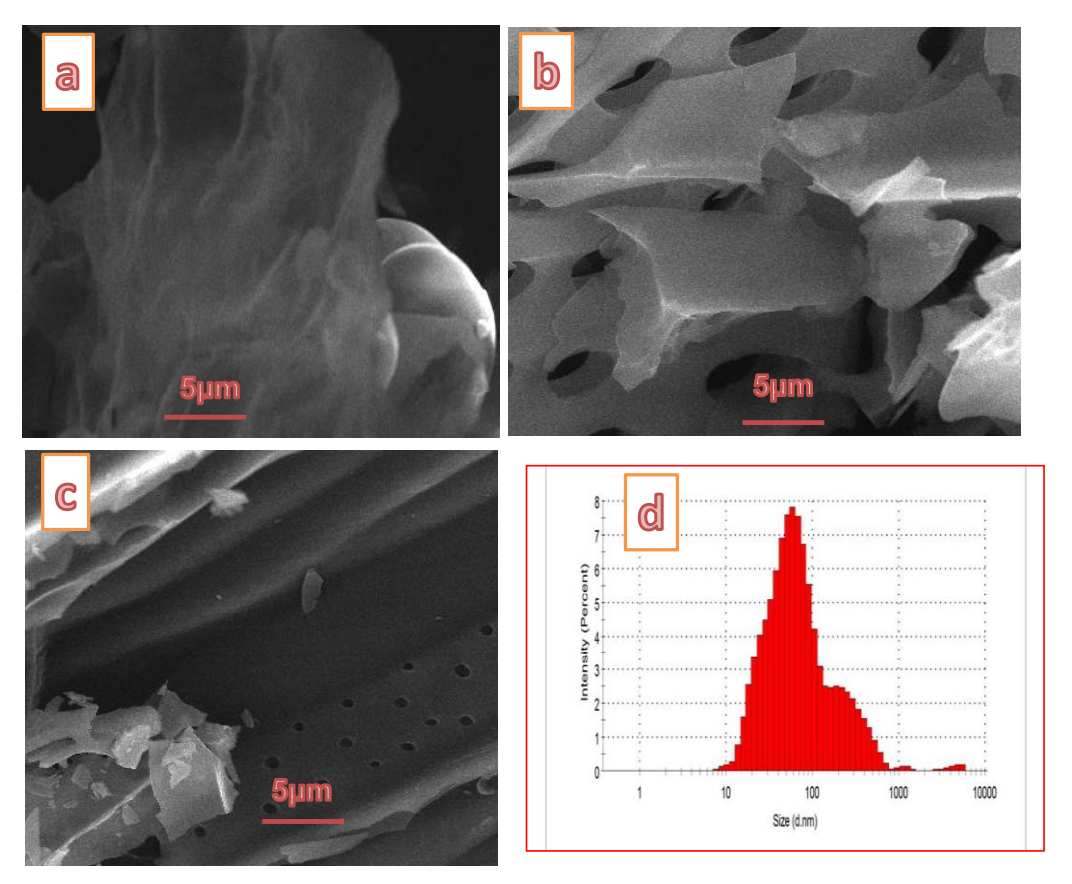


Fig. 2. SEM images of (a) raw USPW, (b) MSPW before adsorption, (c) MSPW after MB adsorption, and (d) particle size of MSPW

Figure 3 depicts the FT-IR spectra of MB and MSPW with and without MB adsorption, ranging from 400 to 4000 cm⁻¹. FT-IR analysis of methylene blue (Table 3) shows peaks of –NH/–OH overlapped stretching vibration at 3622, 3514 and 3405 cm⁻¹, while asymmetric stretching of C–H in alkane groups was observed at 2968 cm⁻¹ (Abdulmohsen and Maqsood 2019).

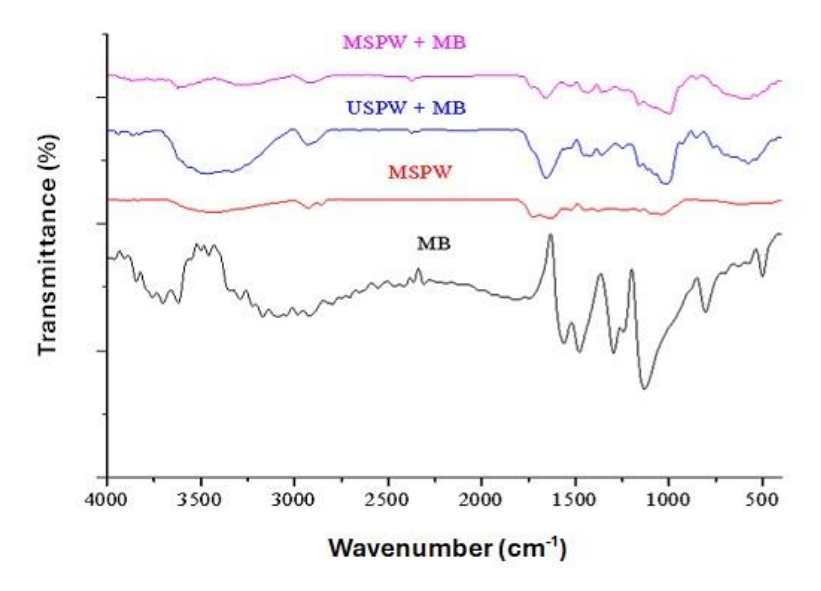


Fig. 3. FT-IR spectra of MSPW, MSPW +MB and MB alone

A peak ascribed to C=N was seen at 1622 cm⁻¹, whereas the 1445 and 1536 cm⁻¹ peaks belonged to C-N band of amide II and C=O symmetrical stretching band of carboxyl, respectively (Xia *et al.* 2015). The peaks corresponding to –CH₂ or –CH₃ stretching were noticed at 1436 to 1345 cm⁻¹, while the of peak of –C–N was noticed at 1255 cm⁻¹ (Abdulmohsen and Maqsood 2019). The bands seen at 1148 and 856 cm⁻¹ denote the band of N-H and C-N of amide III band (Xia *et al.* 2015). For carbonized SPW, the spectra showed the presence of negatively charged binding sites such as cyano, carbonyl, amine, and hydroxyl groups. The bands appearing at 3560 and 3485 cm⁻¹ correspond to -NH and -OH stretching, whereas the bands observed between 1644 and 1652 cm⁻¹ are due to C=O and C=C stretching (Ofudje *et al.* 2014). Symmetric stretching of CH₂ was detected at 1487 cm⁻¹, whereas that of C-O stretching was assigned to the stretch between 1157 and 1182 cm⁻¹ (Ofudje *et al.* 2014, 2019).

After methylene blue had interacted with MSPW ash, significant changes in the FT-IR spectrum were observed. These changes reflect the formation of new bonds or interactions between the functional groups in MB and the surface of the ash leading to peaks shift. For instance, the broad O–H stretching peaks observed in the MSPW around 3560 and 3485 cm⁻¹ in the ash shifted to 3545 and 3360 cm⁻¹ after methylene blue adsorption. This suggests an interaction between the hydroxyl groups on the ash surface and the cationic MB molecules, likely via hydrogen bonding (Ofudje et al. 2019). Similarly the Si-O-Si peak associated with silica at 1025 cm⁻¹ in the biomass ash after the adsorption of methylene blue shifted to 1016 cm⁻¹, thus indicating that the silanol (Si-OH) groups on the ash were interacting with the dye which could occur through electrostatic interactions between the negatively charged silicate groups and the cationic methylene blue molecules (Ofudje et al. 2019). In addition, the peak of C=O seen at 1644 cm⁻¹ in MSPW before the uptake of MB equally shifted to 1625 cm⁻¹, while the peak corresponding to C=C at 1652 cm⁻¹ shifted to 1566 cm⁻¹. The corresponding peak attributed to C-O stretching at 1182 cm⁻¹ shifted to 1130 cm⁻¹ and the peak corresponding to CN stretching at 1035 cm⁻¹ shifted to 1029 cm⁻¹ after MB uptake by MSPW ash suggesting that these groups reacted with methylene blue through ion exchange or surface complexation. This indicates that functional groups such as -OH, -CN, -NH₂, C-O, and C=C are involved in the adsorption process.

MB (cm ⁻¹)	MSPW (cm ⁻¹)	MSPW + MB (cm ⁻¹)	Functional Group Assignment
3622, 3514 and 3405	3560 and 3485	3545 and 3360	-NH and -OH
2968			C–H
	1644	1625	C=O
1622	1652	1566	C=C
1536 to 1445			C=O, C-N of amide II and symmetric band of carboxyl
1255			-C-N stretching
	1182	1130	C-O stretching
1148	1035	1029	CN stretching
	1025	1016	Si-O-Si stretching

Table 3. FT-IR Analysis of MB and SPW Biomass Before and After Adsorption

As shown in Fig. 4, The broad peak observed at 2 theta 23.4° in X-ray diffraction (XRD) analysis of biomass ash typically indicates the presence of amorphous silica.

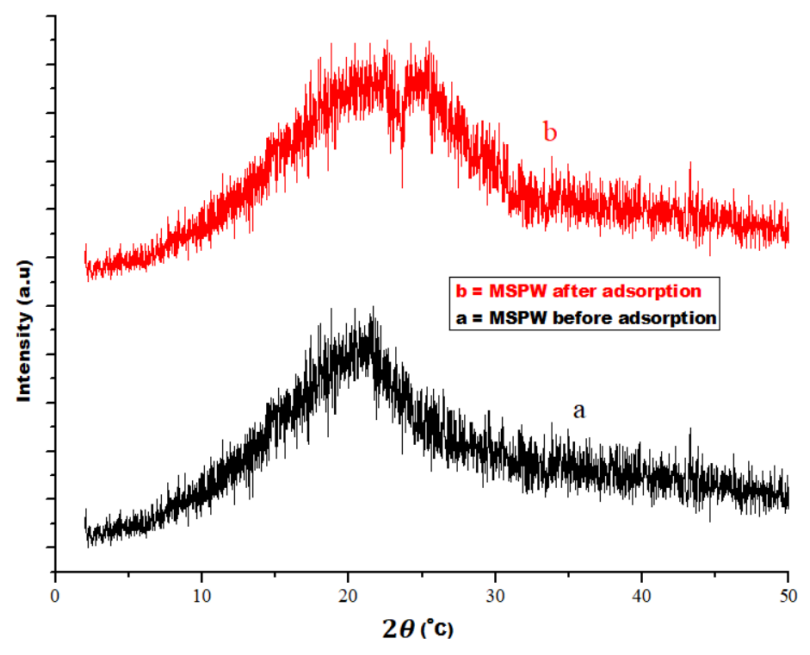


Fig. 4. XRD patterns of SPW and MSPW +MB

After the adsorption of methylene blue onto biomass ash, the XRD analysis shows that the major crystalline phase in biomass ash remained largely unchanged suggesting that methylene blue uptake by the ash molecules does not significantly alter the bulk crystalline structure of the ash. This is expected, since MB adsorption primarily affects the surface of the ash rather than its internal crystal structure. However, an increase in the broad corresponding to amorphous phase in biomass ash at 2 theta = 23.4° extended to 2 thetas = 24.5° after the adsorption process indicating that methylene blue, being an amorphous organic molecule, had adsorbed onto the surface or intercalated into amorphous regions of the ash.

Figure 5 shows the TGA distribution of raw sugarcane peel waste ash. At 67.8 °C and 200.4 °C, the first weight losses of about 1.9% and 4.47% occurred, which correspond to water evaporation in the sample owing to heat treatment (Paulo *et al.* 2011). The heat breakdown of the cellulose in the sample caused a second weight loss of 5.1% at 420.2 °C. At 617.0 °C, the ultimate weight owing to lignin breakdown was recorded. The total weight loss recorded was about 7.6%, with a residue weight of 92.4%, which implies that the ash material has good heat resistance and thermal stability. The high thermal stability of the sugarcane peel waste ash could be attributed to substantial removal of hemicellulose and lignin during the heat treatment process. The decomposition temperatures of hemicellulose, lignin, and cellulose, according to Tasar (2022) and David *et al.* (2020), are 200 to 315, 315 to 400, and 160 to 900 °C, respectively.

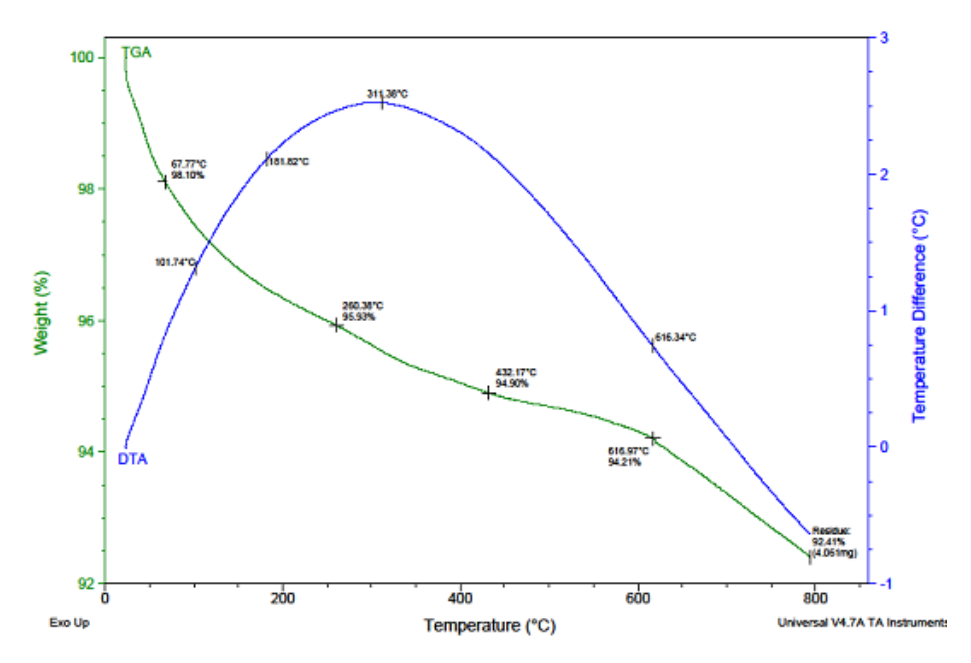


Fig. 5. TGA/DTA Analysis of SPW

Impact of Contact Time and MB Initial Concentration

The impact of time on the adsorption ability of sugarcane peel waste at various MB initial concentrations was studied in a sequence of experiments, as represented in Fig. 6. The quantity (mg/g) of adsorbed MB increased with increasing contact time. As the duration of contact was raised from 5 to 80 min, the amount of MB adsorbed at 25 mg/L rose from 1.45 to 7.60 mg/g and from 11.30 to 22.60 mg/g by adjusting MB concentration to 100 mg/L. When MSPW was used, maximum amounts of MB adsorbed of 9.30 and 33.21 mg/g were attained at 100 mg/L by raising the contact time from 5 to 60 min. After contact times of 60 and 80 min, equilibrium was attained for the two adsorbents, and the amount of MB adsorbed did not increase any further. The MB uptake by SPW was brisk during the first few minutes of contact time, but it became sluggish when the reaction reached equilibrium. This is attributed to empty active sites available on the surface of SPW at the start of the reaction; however, as the adsorption process progressed, these unoccupied centers were occupied by MB particles, thus slowing down the adsorption process. A related account has been documented previously (Cui *et al.* 2019; Puchongkawarin *et al.* 2020).

The report of Ibrahim *et al.* (2014) stated that attaining equilibrium time is a function of the adsorbent structure and nature of the dyes. The role of MB concentration in the uptake process at several reaction times is shown in Fig. 6. The quantity of eliminated MB surged with rise in dye concentration. Reports from the works of Al-Ghouti and Al-Absi (2020), Aluigi *et al.* (2014), and Adeogun *et al.* (2013) came to similar conclusions, and this was ascribed to the surge in the driving force of the pollutant to cross the surface barrier and adhere to the adsorbent surface.

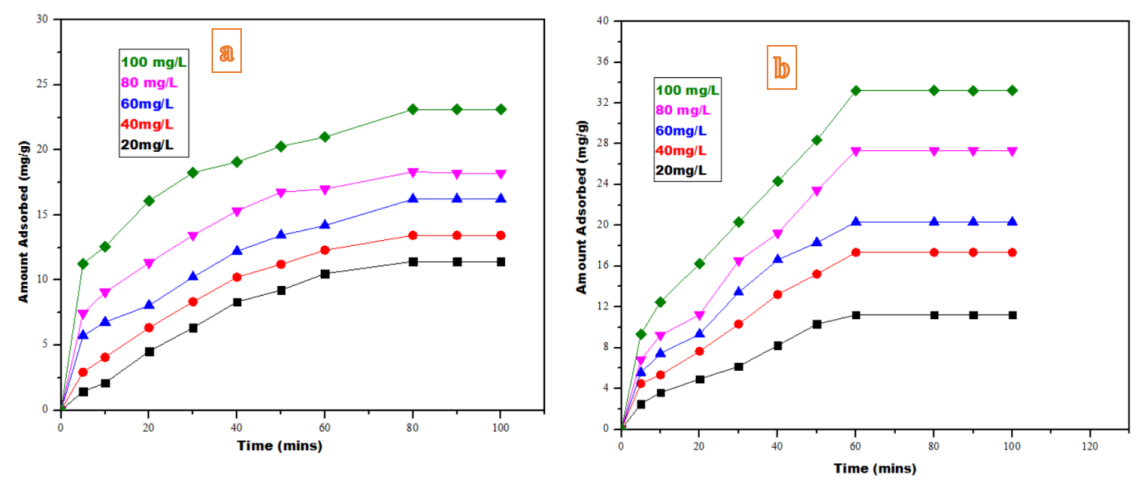


Fig. 6. Effect of reacting time and MB initial concentration by (a) USPW and (b) MSPW at temperature of 45 °C and 55 °C, SPW dosage of 15 mg and pH of 4

Study on the Impact of SPW Dosage

The impact of SPW dosage at different dosages between 10 and 30 mg is represented in Fig. 7. The percentage of MB removed increased as the SPW content increased. When using unmodified SPW, the percentage removal rose from 49.0 to 67.4%, and when treated SPW was utilized, the removal percentage rose from 55.8 to 83.7% when USPW amount was raised from 5 to 15 mg. Upon increasing the adsorbent concentration above 20 mg, there was no noticeable increase in the sorption percentage; thus, a mass of 15 mg was chosen for subsequent experiments. The accessibility of more receptor sites on the adsorbent surface, coupled with a large surface area, may account for the initial increase in the sorption percentage. As more MB is adsorbed by the biomass, a limit was attained where saturation occurs, due to lower sorption effectiveness, as noticed at greater adsorbent concentrations (Adeogun *et al.* 2013; Ofudje *et al.* 2013).

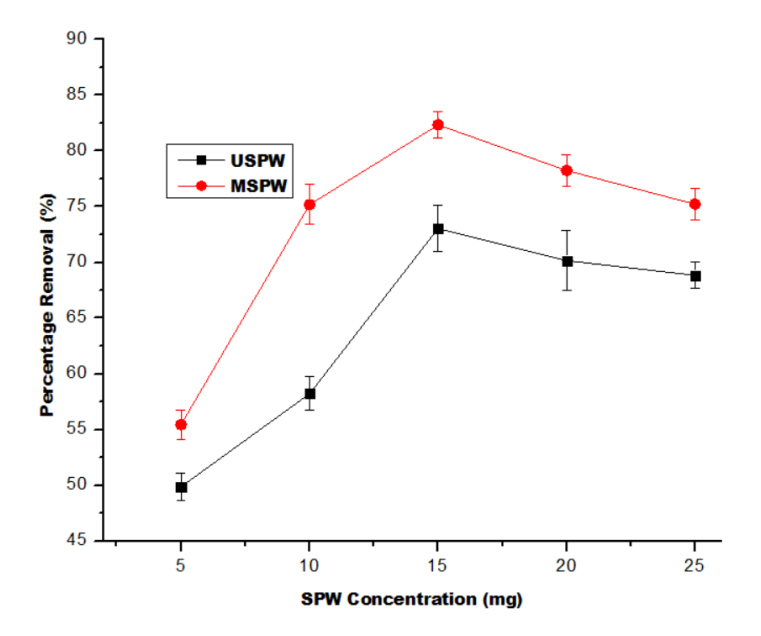


Fig. 7. Effect of SPW dosage at temperature of 45 °C and 55 °C, MB concentration of 100 mg/L, pH of 6, reacting time of 80 and 60 min for USPW and MSPW, respectively

Impact of pH

The chemical behavior of both the sorbent and adsorbate varies with the solution pH, making pH an essential determinant in the elimination of pollutants. Studies were performed to investigate the impact of pH on the sorption of pollutants (Fig. 8).

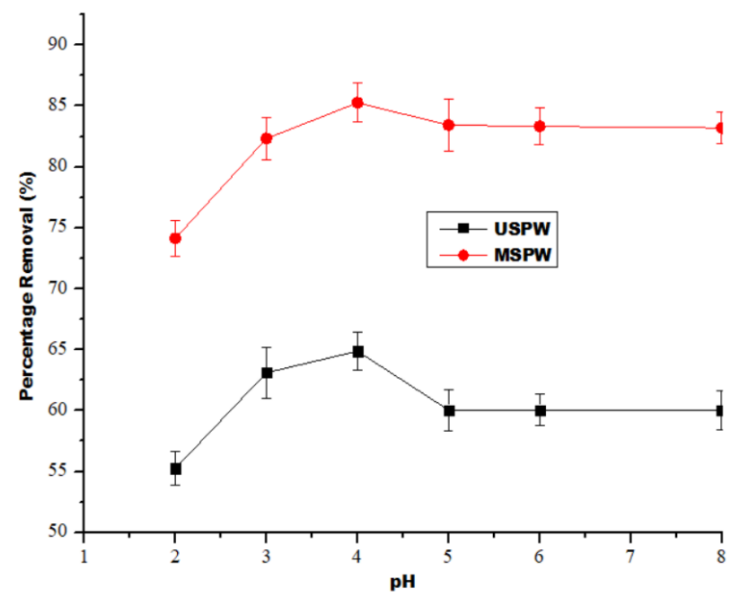


Fig. 8. Effect of solution pH at temperature of 45 °C and 55 °C, SPW dosage of 15 mg, initial concentration of MB at 100 mg/L, reacting time of 80 and 60 min for USPW and MSPW respectively

When untreated SPW was used, the percentage of adsorption rose from 55.6 to 62.4% as the pH was increased from 2.0 to 4; however, when MSPW was used, the sorption percentage rose from 72.5 to 85.1%. At a solution pH of 4.0, the maximum MB

absorption was achieved, and there was no discernible surge in the MB amount removed. To further examine the role of pH, the point of zero charge (pHzPC) was calculated and it was observed that USPW and MSPW had pHzPC values of 3.68 and 5.80, respectively (Table 1). The SPW surface is projected to be negatively charged above this pH value and positively charged below it (Adeogun *et al.* 2013; Ofudje *et al.* 2013).

As a result of the increase in electrostatic attraction involving the negatively charged surface and the cationic methylene blue surface, the uptake of MB by SPW is undoubtedly boosted at pH 6.0 (Adeogun *et al.* 2012; Ofudje *et al.* 2013). At low pH, competition between protons and MB towards the empty sites of SPW surface resulted in lower MB adsorption; however, as the pH rose, the SPW surface was less protonated, thus weakening the rivalry between the proton and MB for empty sites of SPW surface. This resulted in an increased amount of MB adsorbed by the adsorbent, thus suggesting an electrostatic attraction mechanism (Aluigi *et al.* 2014; Ouyang *et al.* 2015).

Temperature Impact

Figure 9 depicts the temperature impact on the sorption of MB by both the adsorbents. The experimental findings revealed that the sorption process was temperature dependent. Temperature improved the sorption effectiveness. At 45 and 55 °C, the maximum sorption capacity of 65.4 and 81.2% was reached for USPW and MSPW, with no further noticeable increase in the sorption capacity. The fact that the sorption efficiency increased with temperature suggests that the sorption process was endothermic (Ofudje *et al.* 2015; Mashkoor *et al.* 2020). The following assumptions can be used to explain this: First, as the temperature increases, MB molecules gain more kinetic energy, which improves the movement of MB particles onto the biomass surface, leading to a rise in the capacity of adsorption of the biomass. Second, an increase in temperature could cause internal swelling of the sorbent, which can enhance dye molecule penetration across the boundary layer on the biomass surface (Turgay *et al.* 2012; Mashkoor *et al.* 2020).

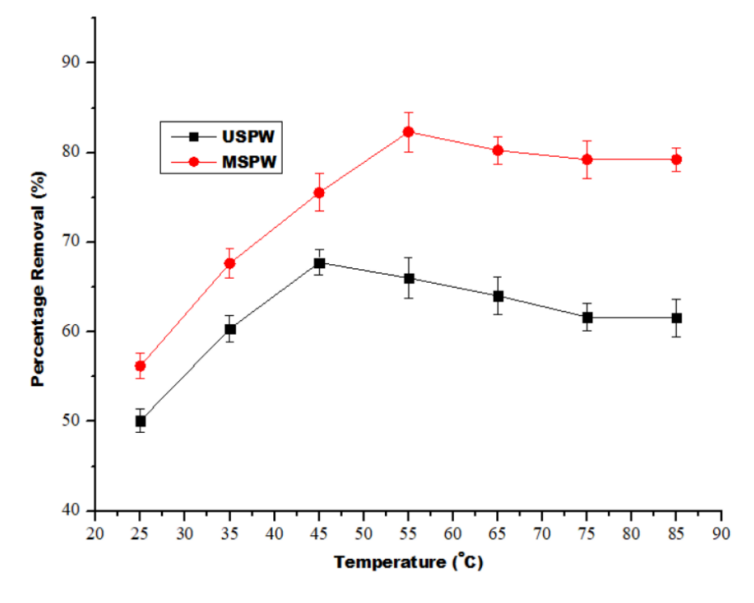


Fig. 9. Effect of temperature at SPW dosage of 15 mg, initial concentration of MB at 100 mg/L, solution pH of 4.0, contact time of 80 and 60 min for USPW and MSPW respectively

Kinetics Study

The adsorption mechanism was investigated using three different kinetic models, including the Lagergren pseudo-first-order (PFO), the pseudo-second-order (PSO), and the intraparticle diffusion kinetic models, to fit the kinetic adsorption data. The linear form of the PFO equation was provided as follows (Turgay *et al.* 2012; Ofudje *et al.* 2022a),

$$In(q_e - q_t) = Inq_e - k_1 t \tag{3}$$

where the parameters q_e and q_t denote MB amount adsorbed at equilibrium (mg/g) and at time t in seconds, respectively, k_l denotes the LPFO constant in mins⁻¹ and its values are obtained via the linear plots of $In(q_e - q_t)$ versus t (Fig. 10a). Table 4 presents the parameters for the PFO model.

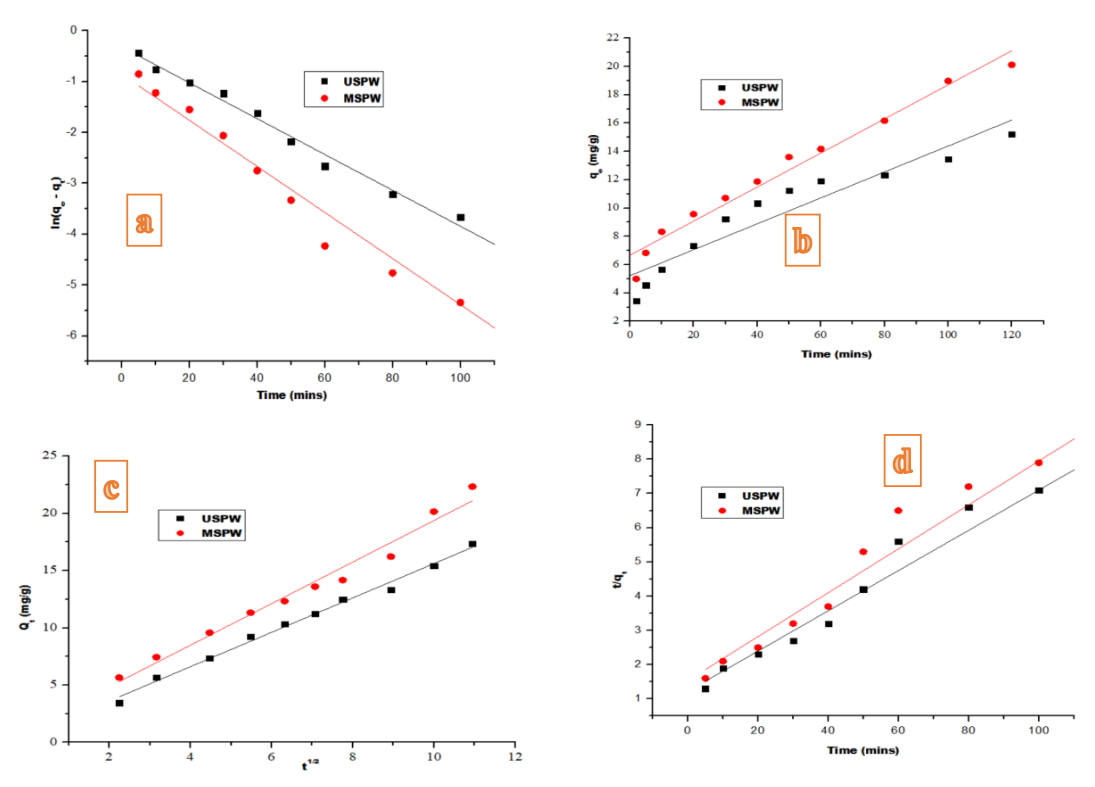


Fig. 10. Kinetic models of (a) pseudo-first order, (b) pseudo-second order, (c) intraparticle and (d) Elovich MB adsorption by USPW and MSPW at temperature of 45 °C and 55 °C, concentration of 100 mg/L, and pH of 4.0

The kinetic representation of the PSO is expressed as follows (Turgay *et al.* 2012; Mashkoor, *et al.* 2020),

$$\frac{t}{q_t} = \frac{1}{k_2 q_e^2} + \frac{1}{q_e} t \tag{4}$$

where the PSO constant is denoted as k_2 , and q_e and q_t are as stated above. k_2 values were determined from the intercept of the plots of t/q_t versus t (Fig. 10b). The constant's values obtained are provided in Table 4.

The intraparticle diffusion equation is given by Eq. 5 (Ofudje *et al.* 2022a; Adeogun *et al.* 2012),

$$q_t = k_p t^{0.5} + I \tag{5}$$

where k_p defines the constant of intraparticle diffusion (mg g $^{-1}$ min $^{-0.5}$) and I gives the boundary layer of the thickness of the adsorbent surface with a larger intercept, suggesting a greater boundary layer effect (Adeogun *et al.* 2013; Ofudje *et al.* 2013). A linear plot of q_t versus $t^{0.5}$ is presented in Fig. 10c, and Table 4 presents the physical parameters.

The Elovich kinetics model given as Gulay and Mehmet (2018) and Muedi *et al.* (2022),

$$q_t = \frac{1}{\beta} \ln(1 + \alpha \beta t) \tag{6}$$

where α and β stand for Elovich's constants denoting the adsorption rate at the initial stage (mg/g/min) and the desorption constant (g/mg) respectively. Figure 10d, and Table 4 present the physical parameters.

Fitness of Kinetic Model

Statistical sum of error squares (SSE, %) was used to investigate the most appropriate kinetic model that best described the data (Ofudje *et al.* 2022a),

% SSE =
$$\sqrt{\frac{((Q_{(exp)} - Q_{(Cal)})/Q_{exp}}{N-1}}$$
 (7)

where N denotes the number of data points, and with a small value of %SSE coupled with high R^2 values, the more appropriate the model.

For the USPW, the coefficients of determination (R²) from the PSO model were greater than those of the PFO model. In addition, the adsorption capacity (q_{exp}) with the theoretical adsorption capacity (q_{cal}) values, the PSO model showed better agreement, as shown in Table 4. However, for MSPW, the kinetic data fitted well with PFO because of the high values of R^2 and the closeness of the $q_{\rm exp}$ with $q_{\rm cal}$. Thus, the uptake of MB by the untreated and treated SPW was better represented by the PSO and PFO models, respectively (Turgay et al. 2012; Mashkoor et al. 2020). This is also supported by the low %SSE values obtained, as shown in Table 4. From the characterizations carried out (SEM, FTIR and XRD), it's obvious that the microstructure of the USPW was different from that of the MSPW. Since the reactivity of the adsorbent is a function of its component, the mechanism of adsorption of MB by USPW is expected to be different from that of MSPW. In addition, the adsorption data for MB were consistent with those of the intraparticle diffusion model, with $R^2 > 0.9$. The dye adsorption mechanism can be explained in three stages: (1) movement from the solution through the border film onto the adsorbent surface, (2) crossing over of the adsorbent exterior surface to the adsorbent interior sites through pore diffusion, and (3) adsorbate diffusion to the active centers through a surface solid diffusion mechanism (Aluigi et al. 2014; Al-Ghouti and Al-Absi 2020). The values of α for USPW and MSPW (Table 4) ranged from 2.435 to 5.282 and from 3.122 to 6.124, whereas that of β ranges from 0.105 to 0.557 and 0.112 to 0.853 respectively. The R² values were found to be in the range of 0.955 to 0.982 for USPW and 0.976 to 0.998 in the case of MSPW which suggests the suitability of this model in predicting the kinetic data of MB.

_bioresources.cnr.ncsu.edu

Table 4. Parameters from Kinetics Analysis of the Adsorption of MB by USPW and MSPW

		USPW					MSPW				
Pseudo-first order	C₀ (mg/L)	20	40	60	80	100	20	40	60	80	100
	Q _{e exp} (mg g ⁻¹)	8.002	11.201	15.015	18.130	22.600	12.206	18.102	25.000	29.013	32.210
	Q _{e cal} (mg g ⁻¹)	13.016	16.063	19.107	22.038	28.015	11.031	17.024	26.213	30.116	33.018
	k ₁ (min ⁻¹)	1.015	1.237	1.351	1.601	2.010	2.016	2.022	3.031	3.042	4.015
	R ²	0.984	0.987	0.929	0.979	0.967	0.998	0.996	0.998	0.999	0.996
	%SSE	0.083	0.310	0.221	0.402	0.601	0.001	0.006	0.003	0.014	0.041
Pseudo-second order	Q _{e cal} (mg g ⁻¹)	9.212	13.105	16.204	19.103	22.110	10.104	15.205	22.109	25.032	39.103
order .	k ₂ (g mg ⁻¹ min ⁻¹)	0.129	0.151	0.257	0.273	0.411	0.522	1.215	1.501	1.619	1.790
	R ²	0.995	0.997	0.995	0.989	0.995	0.968	0.958	0.949	0.968	0.988
	%SSE	0.012	0.015	0.024	0.003	0.060	0.124	0.261	1.209	0.907	1.013
Intra-particle diffusion	K _{1d} (mg g ⁻¹ min ^{-0.5})	3.113	5.221	7.101	9.022	11.102	2.103	3.102	5.124	8.131	10.162
amusion	C ₁ (mg g ⁻¹)	-0.204	-0.322	-0.601	-1.211	-3.203	-0.212	-0.601	-1.208	-1.503	-1.492
	R ²	0.966	0.977	0.988	0.946	0.928	0.962	0.940	0.983	0.967	0.988
	α	2.435	3.071	4.344	4.631	5.284	3.122	3.528	4.565	5.201	6.124
Elovich	β	0.105	0.128	0.241	0.341	0.557	0.112	0.134	0.355	0.501	0.853
	R ²	0.976	0.966	0.982	0.977	0.955	0.986	0.988	0.976	0.987	0.998

9206

Equilibrium Studies

Freundlich, Langmuir, Temkin, and Dubinin-Radushkevich (D-R) isotherms were employed to assess the MB equilibrium data for sugarcane peel waste (Turgay *et al.* 2012; Mashkoor *et al.* 2020).

The Langmuir isotherm is denoted in Eq. 8,

$$\frac{c_{\ell}}{q_{\ell}} = \frac{1}{qL_{max}\frac{c_{\ell}}{q_{max}}} \tag{8}$$

where the parameter q_e was previously defined above, q_{max} (mg/g) is the monolayer capacity of adsorption, and the Langmuir constant in mg/L is given as K_L . The values of K_L and q_{max} were estimated from the intercept and slope of the linear plots of C_e/q_e against C_e , as shown in Fig. 11, and Table 5 lists the physical parameters. To check whether the adsorption is favorable, the Langmuir separation factor R_L was computed as follows,

$$R_L = \frac{1}{(1+bC_0)} \tag{9}$$

where b denotes the Langmuir constant. When R_L is above 1, the adsorption is unfavorable; however, when RL lies between 0 and 1, it is said to be favorable (Adeogun *et al.* 2013).

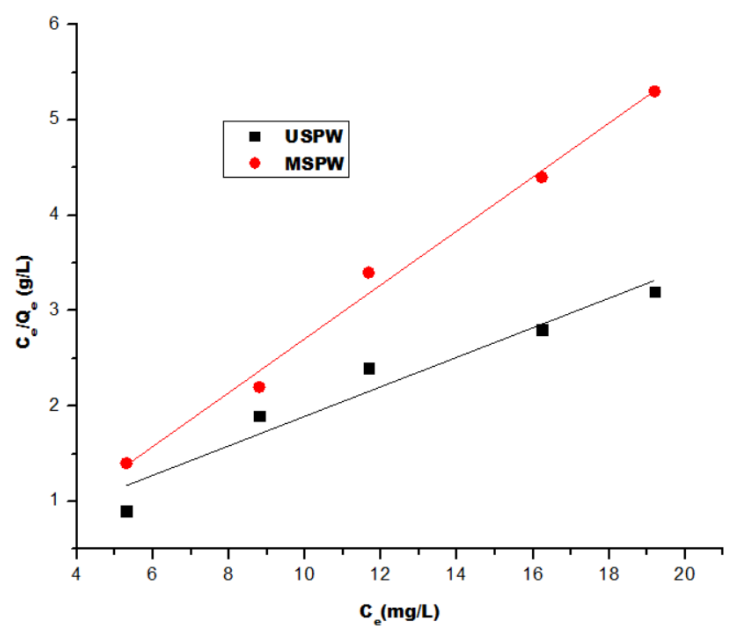


Fig. 11. Langmuir isotherms plot for MB sorption by USPW and MSPW

The Freundlich isotherm is depicted as follows (Adeogun *et al.* 2013; Mashkoor *et al.* 2020),

$$Inq_e = InK_F - \frac{1}{n}InC_e \tag{10}$$

In Eq. 10, the adsorption capacity is represented by K_F , and the intensity of adsorption is given by n. The values of K_F and n were estimated from the linear plots of Inq_e against InC_e (see Fig. 12), and Table 5 presents the physical parameters.

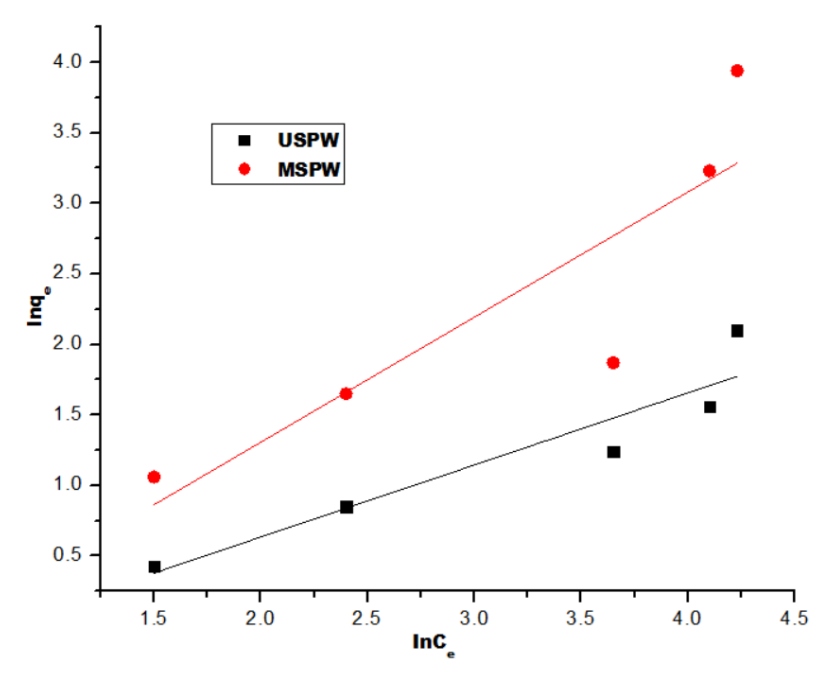


Fig. 12. Freundlich isotherms plot for MB sorption by USPW and MSPW

The Temkin isotherm which adopted a multilayer adsorption pattern of interactions between the adsorbent and adsorbate, but neglect the medium by little or greater concentration, can be expressed as follows (Wu et al. 2020; Ofudje et al. 2022a),

$$Q_e = \left(\frac{RT}{\beta}\right) \ln K_T + \left(\frac{RT}{\beta}\right) \ln C_e \tag{11}$$

where the universal gas constant is denoted by R (J/(mol K), β denotes the adsorption heat constant in J/mol (see Fig. 13a), T stands for temperature (K), and Table 5 presents the physical parameters.

The Dubinin-Radushkevich (D-R) model can be showcased as follows (Gulay and Mehmet 2018; Wu *et al.* 2020; Muedi *et al.* 2022),

$$Inq_e = Inq_m - \beta \epsilon^2 \tag{12}$$

with $q_{\rm m}$ denoting the maximum adsorption capacity (mol/g), while the Polanyi potential of the adsorption process is given as ϵ in mol²/j² and expressed by Eq. 13.

$$\in = RTIn(1 + \frac{1}{C_{\varepsilon}}) \tag{13}$$

The adsorption free energy of the adsorption process which is denoted as E (kJ/mol) is expressed in Eq. 14.

$$E = \frac{1}{\sqrt{2K_{DR}}} \tag{14}$$

Figure 13b and Table 5 present graphs and the physical parameters of the D-R model.

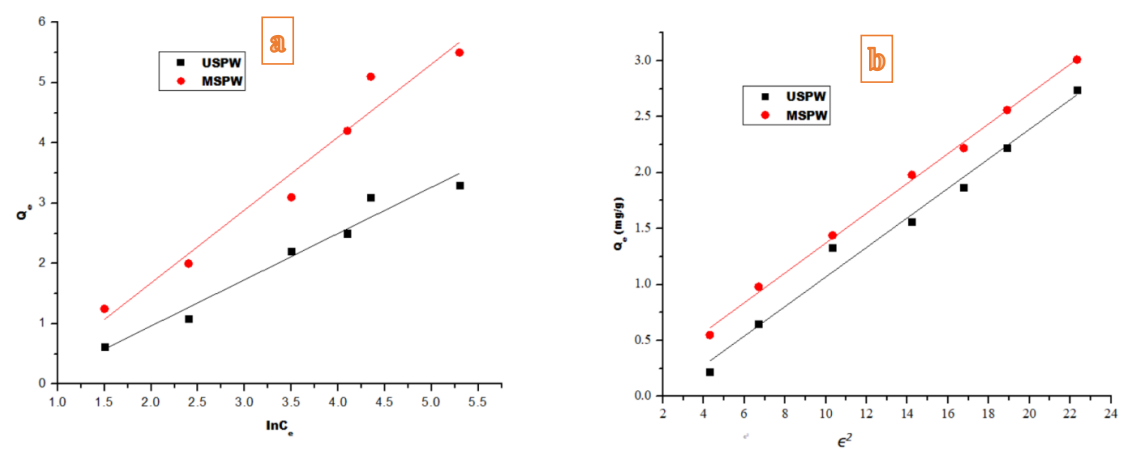


Fig. 13. (a) Temkin isotherm and (b) Dubinin-Radushkevich (D-R) isotherm models by USPW and MSPW for the adsorption of MB

The Freundlich isotherm produced better results for USPW, judging from the coefficient of determination (\mathbb{R}^2) values and adsorption capacities of the isotherms tested, while the Langmuir isotherm gave better fits for MSPW. This shows that MB sorption onto the surface of USPW has heterogeneous surface energies, whereas that of MSPW provided homogeneous surface energies. Values of 1/n are less than unity, implying successful adsorption of MB by the USPW and MSPW surfaces (Turgay *et al.* 2012; Ofudie *et al.* 2015; Mashkoor and Nasar 2020).

Table 5. Isotherm Constants in Absorption by USPW and MSPW

Isotherms	Parameters	USPW	MSPW
	q _{max} (mg/g)	24.451	32.317
l	K _L (mg/L)	0.024	0.213
Langmuir	R∟(mg/L)	0.221	0.518
	R ²	0.887	0.994
	K₅ (mg/g)	12.418	20.051
Freundlich	1/n	0.135	0.241
	R ²	0.987	0.929
Tambin	β (mg/g)	5.601	8.214
Temkin	R ²	0.968	0.979
	q _m (mg/g)	4.205	6.883
Dubinin-Radushkevich	E (kJ/mol)	31.014	4.642
(D–R)	β (mol kJ ⁻¹) ²	0.251	0.482
- •	R^2	0.946	0.987

Note: SPW dosage of 20 mg, temperature of 45 $^{\circ}$ C, reacting time of 60 and 80 min for USPW and MSPW, respectively

The highest adsorption capacities of untreated sugarcane peel waste and treated sugarcane peel waste for MB were 24.5 and 35.3 mg g⁻¹, respectively, as predicted by the Langmuir isotherm. Furthermore, the R_L values were 0.221 and 0.518, indicating a favorable process of adsorption. As revealed in Table 6, the maximum adsorption capacity obtained revealed that the tested adsorbents in this study performed better than other adsorbents, as previously documented in the literature, which further indicated the usability of sugarcane peel waste ash as an effective adsorbent for MB removal. The

coefficients of determination obtained when the Temkin isotherm was deployed were 0.968 and 0.979 for USPW and MSPW respectively, and this implies that this model can be employed in explaining the equilibrium data of MB adsorption by the two adsorbents. The β values obtained were 5.60 and 8.21 mg/g for USPW and MSPW, respectively, indicating that more of MB was adsorbed by the modified adsorbent. The obtained upper limit adsorption capacity values for the USPW and MSPW were 4.206 and 6.883 mg/g, whereas the R^2 values were 0.946 and 0.987, respectively.

Furthermore, the value of E from the D-R model can be deployed to elucidate the adsorption mechanism. If E is <8 kJ/mol, physisorption is controlling the adsorption process but if, the value of E is between 8 and 16 kJ/mol, the adsorption process is said to be ion exchange, whereas when value falls within the range of 20 to 40 kJ/mol, it is classified as chemisorption (Wu *et al.* 2020; Gulay and Mehmet 2018; Muedi *et al.* 2022). For the adsorption of MB by USPW, the E value found was 31.0 kJ/mol, which suggests chemical adsorption; however, in the case of MSPW, the value of E found was 4.642 kJ/mol confirming physical adsorption process.

Table 6. Comparative Analysis of the Maximum Adsorption Capacity of Sugarcane Peel Waste with Related Adsorbents in Literature

Biomaterials	Activating Agent	Maximum Adsorption capacity (mg/g)	References		
Bali cow bones		7.200	Neolaka et al. (2023)		
kaolin		23.000	Yavuz and Saka, (2013)		
Shea cake	Chemical- H ₃ PO ₄	32.270	Ibrahim <i>et al.</i> (2014)		
Cotton cake	Chemical- H ₃ PO ₄	32.330	Ibrahim <i>et al.</i> (2014)		
N-maleyl chitosan/P(AA-co-VPA)		50.180	Nakhjiri <i>et al.</i> (2018)		
Poly (vinyl alcohol)/Vitamin C-mu		16.844	Mallakpour <i>et al</i> .		
walled carbon nanotubes compos			(2019)		
Yellow passion fruits peel		6.800	Pavan <i>et al</i> . (2008)		
Fly ash		50.27	Wang et al. (2023)		
modified biochar material		5.018	Hoslett et al. (2020)		
Polyethylene Terephthalate Nanofiber-Multi-Walled Carbon Nanotube Composite		7.047	Essa et al. (2022)		
Untreated sugarcane biomass	-	24.457	This study		
Treated sugarcane biomass	Physical	32.315	This study		

Study on Thermodynamics

The changes in enthalpy (ΔH) , free energy (ΔG) , and entropy (ΔS) during the adsorption process are listed in Table 6. The Van't Hoff model provides the relationship between ΔG , ΔH , and ΔS at a particular temperature, as described below (Adeogun *et al.* 2013),

$$InK_C = -\frac{\Delta H^o}{RT} + \frac{\Delta S^o}{R} \tag{15}$$

where K_C denotes the equilibrium constant and defines the correlation between the adsorbed amounts of MB (q_e) and the equilibrium concentration (C_e) , and R denotes the

gas molar constant, which is given by Eq. 16 (Mashkoor et al. 2020).

$$K_C = \frac{q_e}{C_e} \tag{16}$$

The values of ΔH and ΔS were deduced through the graphical representation of InK_C versus I/T, as shown in Fig. 14, while ΔG was deduced using the relation below:

$$\Delta G = -RTInK_C \tag{17}$$

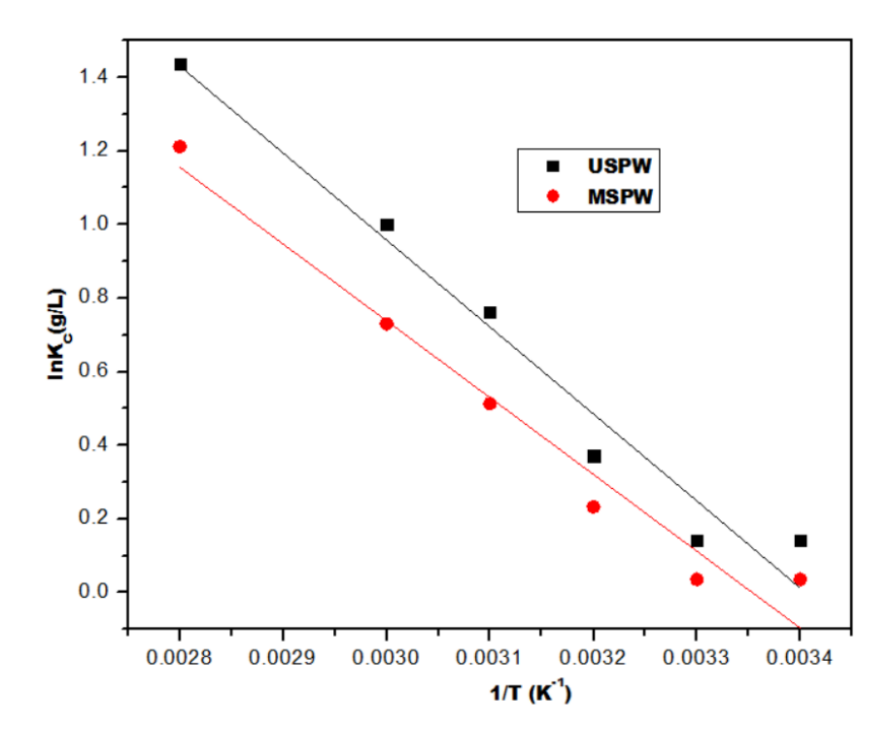


Fig. 14. Thermodynamics plots of MB by SPW and MSPW

Table 7. Thermodynamic Constants in the Uptake of MB by SPW

	USPW MSPW					
(K)	ΔG	ΔΗ	ΔS	ΔG	ΔΗ	ΔS
	(kJmol ⁻¹)					
298	- 440.950			- 463.210		
303	-51.901	91.150	20.220	-631.612	17.240	32.100
308	-658.601			-726.014		
313	-763.251			-806.306		
323	-813.230			-931.104		

The values of ΔG obtained were negative, confirming the feasibility of the process of MB uptake as well as the spontaneity of the process (Table 7). The negativity of ΔG increased with temperature, indicating that at higher temperatures, more pollutants were adsorbed onto the SPW surface. The estimated values of ΔH and ΔS were 91.2 and 20.2 kJ mol⁻¹K⁻¹ for untreated SPW and 17.2 kJ and 32.1 kJ mol⁻¹K⁻¹ for treated SPW, respectively. Because ΔH was positive, it indicates that MB adsorption by the two adsorbents was endothermic in nature (Ofudje *et al.* 2014, 2019). The ΔH values can be engaged to predict the nature of the adsorption process to either be physical (2.1 to 20.9 kJ/mol) or chemical adsorption (80 to 200 kJ/mol) (Gupta *et al.* 2013). In this work, the

values of ΔH suggest that MB adsorption by untreated and treated SPW can be classed as chemical and physical in nature, respectively. Furthermore, as ΔS is positive, it signifies a surge in the degree of randomness of the adsorption process.

Reusability of SPW

The future applications of the adsorbent, which indicates its industrial application, were tested using a 0.1M solution of NaOH solution as the eluting agent (Neolaka *et al.* 2023). The MB-loaded SPW was eluted at 80 and 60 min contact times for USPW and MSPW in five reusability cycle times, as depicted in Fig. 15. The amount of desorbed MB was measured using a UV-visible spectrophotometer. The desorption percentages of USPW and MSPW after five times of reusability were 74.2, 69.3, 65.4, 57.2, and 54.4% and 82.2, 77.4, 69.6, 64.3, and 59.2%. The study showed that the desorption efficiency of the adsorbent towards MB decreased with an increase in the reusability time, although SPW can be successfully applied more than once in the adsorption of MB.

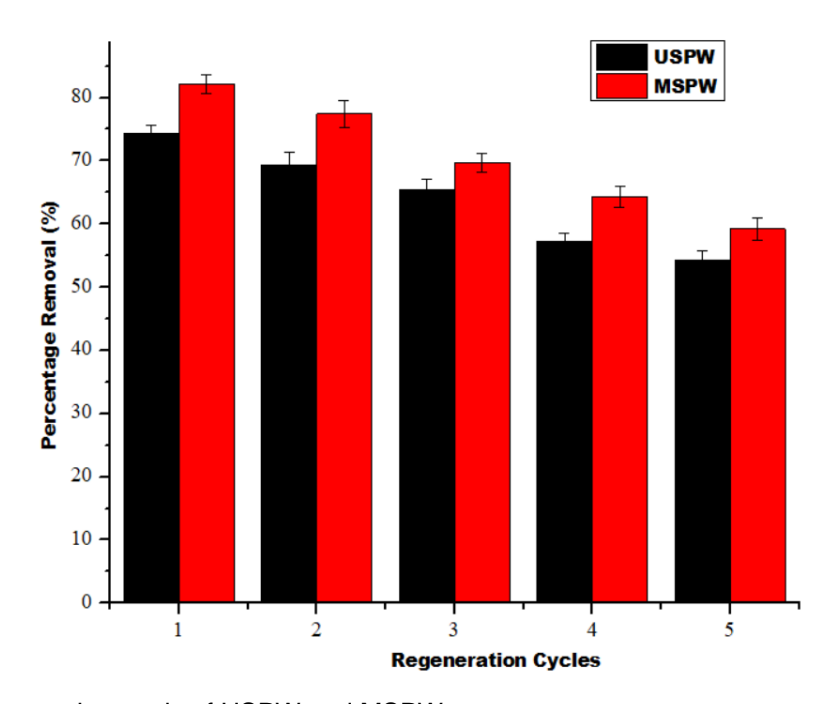


Fig. 15. Regeneration study of USPW and MSPW

Mechanism of MB Adsorption by SPW

To further explain the mechanism of MB adsorption by USPW and MSPW, the adsorbent was characterized. Based on the FT-IR surface assessment of the adsorbent, it was discovered that it was mainly composed of functional groups such as-OH,-CN,-NH2, C-O, and C=C, which are negatively charged and can easily be trapped by positively charged MB molecules via electrostatic attraction. The SPW surface according to the pHzpc study was negatively charged above the pH of 5.0, resulting in an increase in electrostatic attraction with the cationic methylene blue surface, resulting in undoubtedly adsorption of MB particles onto the adsorbent surface, thus corroborating the electrostatic attraction mechanism suggested earlier by FT-IR analysis. Jia *et al.* (2016) reported that the negative charge of chemical biomass ash spheres obtained *via* the hydrothermal synthesis of poly(vinyl alcohol) microspheres in aqueous media attracted MB molecules,

which were positively charged as a result of strong electrostatic interactions. A schematic diagram of the proposed adsorption mechanism of MB by the SPW is shown in Fig. 16.

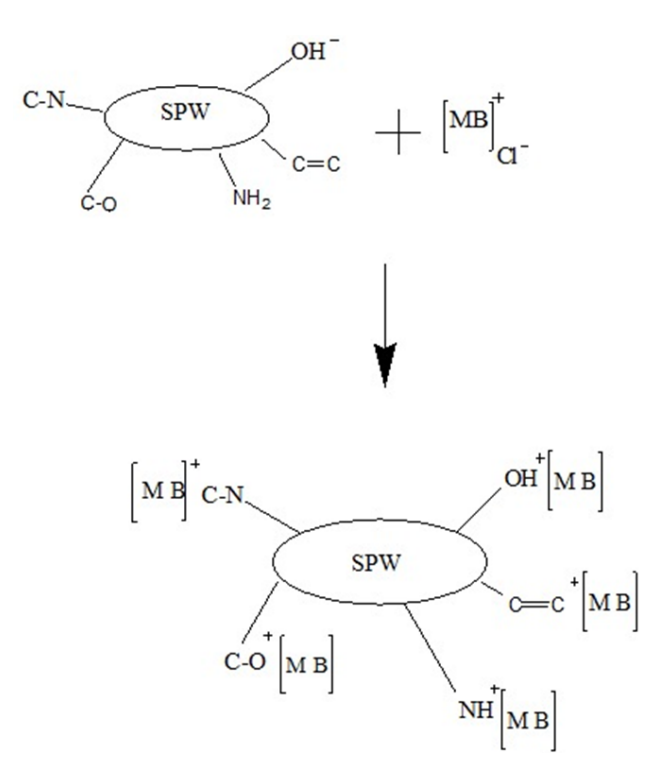


Fig. 16. Schematic diagram showing the mechanism of adsorption of MB by SPW

Estimating the Cost of Producing Sugarcane Peel Waste Adsorbent

In estimating the cost of using unmodified and heat-treated sugarcane peel waste as adsorbents for MB removal in water treatment, there are few things that need to be taken into consideration, and these are:

- The value of sugarcane peel waste
- The cost of machines (rotational brush, circular knifing, *etc.*) uses for peeling operation of the sugar cane.
- The man hour input.
- Calcination cost
- Cost of chemicals
- Water

The life of a unit mass of the adsorbent powder includes preparation, enhancement, deployment, elution and disposal:

- Sugarcane peel sourcing
- Fabrication compounding, sieving, sizing processes etc.
- Heat treatment (cost of energy per Kg {KWh})
- Deployment method
- Elution cycle (maintenance reusing one time usage)
- Working capital investment

The total capital investment for the proposed adsorbents is given as follows (Fingolo *et al.* 2020; Yashni *et al.* 2020),

$$TCI = WCI + FCE \tag{18}$$

where TCI is the total capital investment, WCI is the working capital investment (6.5% of FCE), and FCE is the estimated fixed capital. The preparation cost of the adsorbent per annual is given as follows (Fingolo *et al.* 2020; Yashni *et al.* 2020),

$$AO_C = C_{RM} + C_{WG} + C_U + C_E \tag{19}$$

where AO_C is the annual operation cost adsorbent preparation, C_{RM} is the cost of materials, C_{U} is the cost of utilities, C_{WG} is the cost of equipment handling, and C_{E} is the extra cost.

Figure 1, which depicts the adsorbent preparation and application, suggests a three stages process. The first stage which has to do with collection of raw materials, washed and pulverization. The second stage entails the preliminary chemical treatment followed by third stage which involves the heat treatment. The fixed capital estimation denotes all equipment purchase and installation, buildings, electrical systems, instrumentation and controls, and construction including the WCC which could be up to 6.5% of FCE (Fingolo *et al.* 2020; Yashni *et al.* 2020). The cost of the raw material is expected to be free (negligible), since the material is obtained from waste. Thus, the production cost of USPW and MSPW in the treatment of 20, 000 m³/year of wastewater is estimated to be 695 USD and 708 USD respectively (Table 8). Though, the cost of fabricating MSPW is a bit greater compared with that of USPW (13 USD greater) which is due to the extra cost of converting the raw material into biomass ash, the modified form of the adsorbent is still much superior since MSPW adsorption capacity is greater when compared with USPW.

Unit Units Quantity **Parameters** Cost Cost price (USD) (USD) **USPW MSPW** Utilities USD/m³ Water 0.0013 20,000 26.00 26.00 0.026 USD/kWh 7,000 N/A **Electricity** 182.00 supply **Others** Maintenance 1.4 % of FCE N/A 220.00 220.00 USD/employee Labour 23.34 280.08 280.08 1 Chemicals Chemicals 6.75 25g 168.75 N/A

Table 8. Techno-economic Assessment of SPW

CONCLUSIONS

The ability of untreated and thermally treated (combusted) sugarcane peel waste (SPW) to eliminate methylene blue (MB) dye in an aqueous medium was tested, and the following findings were derived:

- 1. Biomass ash was successfully produced from sugarcane peel waste.
- 2. The functional group controls MB adsorption onto untreated (USPW) and modified by converting to ash (MSPW) adsorbents.
- 3. For the USPW, the pseudo-second-order (PSO) model provided better fits, whereas the pseudo-first-order (PFO) model showed better agreement with the MSPW.
- 4. The Freundlich isotherm produced better results for USPW, whereas the MSPW adhered to the Langmuir isotherm.

- 5. It was established from the study that MSPW is a better adsorbent in methylene blue dye removal than USPW.
- 6. Thus, agricultural remains derived from sugarcane peel waste can be used as a precursor to produce biomass ash, that could be used as a promising adsorbent in the elimination of methylene blue dye from contaminated wastewater.
- 7. Using sugarcane peel ash as an adsorbent for methylene blue (MB) dye removal can be effective, but it may also come with some limitations. For instance, the adsorption efficiency of sugarcane peel ash can be highly pH-dependent. It can have slower kinetics compared to other materials, and sugarcane peel ash might encounter other contaminants.

ACKNOWLEDGMENTS

This work was supported by Princess Nourah bint Abdulrahman University Researchers Supporting Project number (PNURSP2024R13), Princess Nourah bint Abdulrahman University, Riyadh, Saudi Arabia.

Data Availability Statement

The datasets generated and/or analyzed during this study are available from the corresponding author upon request.

Conflict of Interest

All authors have declared that there are no conflicts of interest.

REFERENCES CITED

- Abdulmohsen, A. A., and Maqsood, A. M. (2019). "Biogenic fabrication of ZnO nanoparticles using *Trigonella foenum-graecum* (Fenugreek) for proficient photocatalytic degradation of methylene blue under UV irradiation," *Journal of Materials Science: Materials in Electronics* 30, 16156-16173. DOI: 10.1007/s10854-019-01985-8
- Adeogun, A. I., Ofudje, E. A., Idowu, M. A., and Ahmed, S. A. (2012). "Biosorption of Cr(VI) ion from aqueous solution by maize husk: Isothermal, kinetic and thermodynamic study," *J. Chem. Soc. Pak.* 34(6), 1388-1396.
- Adeogun, A. I., Idowu, M. A., Ofudje, A. E., Kareem, S. O., and Ahmed, S. A. (2013). "Comparative biosorption of Mn(II) and Pb(II) ions on raw and oxalic acid modified maize husk: kinetic, thermodynamic and isothermal studies," *Appl Water Sci.* 3, 167-179. DOI: 10.1007/s13201-012-0070-1
- Ahmad, A., Khan, N., Giri, B. S., Chowdhary, P., and Chaturvedi, P. (2020). "Removal of methylene blue dye using rice husk, cow dung and sludge biochar: Characterization, application, and kinetic studies," *Bioresource Technology* 306, article 123202. DOI: 10.1016/j.biortech.2020.123202
- Al-Ghouti, M. A., and Al-Absi, R. S. (2020). "Mechanistic understanding of the adsorption and thermodynamic aspects of cationic methylene blue dye onto cellulosic olive stones biomass from wastewater," *Sci Rep.* 10, article 15928. DOI: 10.1038/s41598-020-72996-3

- Aluigi, A., Rombaldoni, F., Tonetti, C., and Jannoke, L. (2014). "Study of methylene blue adsorption on keratin nano-fibrous membranes," *Journal of Hazardous Materials* 268, 156-165. DOI: 10.1016/j.jhazmat.2014.01.012
- Boukhemkhem, A., and Rida, K. (2017). "Improvement adsorption capacity of methylene blue onto modified Tamazert kaolin," *Adsorption Science & Technology* 35(9–10), 753-773. DOI: 10.1177/0263617416684835
- Burtch, N. C., Jasuja, H., and Walton, K. S. (2014). "Water stability and adsorption in metal-organic frameworks," *Chemical Reviews* 114, 10575-10612. DOI: 10.1021/cr5002589
- Cardenas, J. A. G., Garcia, B. E., Aguera, A., Perez, J. A. S., and Agugliaro, F. M. (2020). "Wastewater treatment by advanced oxidation process and their worldwide research trends," *Int. J. Environ. Res. Public Health.* 17, article 170. DOI: 10.3390/ijerph17010170.
- Chen, Q., He, Q., Lv, M., Xu, Y., Yang, H., Liu, X., and Wei F. (2015). "Selective adsorption of cationic dyes by UiO-66-NH₂," *Applied Surface Science* 327, 77-85. DOI: 10.1016/j.apsusc.2014.11.103
- Cui, Y. Y., Zhang, J., Ren, L. L., Cheng, A. L., and Gao, E. Q. (2019). "A functional anionic metal-organic framework for selective adsorption and separation of organic dyes," *Polyhedron* 161, 71-77. DOI: 10.1016/j.poly.2018.12.036
- David, D., Ana U., Raul P., Aitor, B., and Tarja, T. (2020). "Determination of hemicellulose, cellulose, and lignin content in different types of biomasses by thermogravimetric analysis and pseudocomponent kinetic model (TGA-PKM method)," *Processes* 8, article 1048. DOI: 10.3390/pr8091048.
- Ding, Z., Hu, X., Zimmerman, A.R., and Gao, B. (2014). "Sorption and cosorption of lead (II) and methylene blue on chemically modified biomass," *Bioresource Technol.* 167, 569-573. DOI: 10.1016/j.biortech.2014.06.043
- Essa, W. K., Yasin, S. A., Abdullah, A. H., Thalji, M. R., Saeed, I. A., Assiri, M. A., Chong, K. F., and Ali, G. A. M. (2022). "Taguchi L25 (54) approach for methylene blue removal by polyethylene terephthalate nanofiber-multi-walled carbon nanotube composite," *Water* 14, article 1242. DOI: 10.3390/w14081242
- Fingolo, A. C., Klein, B. C., Rezende, M. C., Souza, C. A. S., Yuan, J., Yin, G., Bonomi, A., Martinez, D. S., and Strauss, M. (2020). "Techno-economic assessment and critical properties tuning of activated carbons from pyrolyzed sugarcane bagasse," *Waste Biomass Valorization* 11(8), 1-13. DOI: 10.1007/S12649-019-00774-Y
- Gregorio, C., and Eric, L. (2018). "Advantages and disadvantages of techniques used for wastewater treatment," *Environmental Chemistry Letters*. DOI: 10.1007/s10311-018-0785-9
- Gulay, B., and Mehmet, Y.F. (2018). "Adsorption of Congo Red dye by native amine and carboxyl modified biomass of *Funalia trogii*: Isotherms, kinetics, and thermodynamics mechanisms," *Korean J. Chem. Eng.* 35(3), 1-9. DOI: 10.1007/s11814-018-0033-9
- Gupta, V. K., Pathania, D., Sharma, S., Agarwal, S., and Singh P. (2013). "Remediation and recovery of methyl orange from aqueous solution onto acrylic acid grafted *Ficus carica* fiber: Isotherms, kinetics and thermodynamics" *Journal of Molecular Liquids* 177, 325-334. DOI: 10.1016/j.molliq.2012.10.007
- Gupta, M., Gupta, H., and Kharat, D. S. (2018). "Adsorption of Cu(II) by low cost adsorbents and the cost analysis," *Environ. Technol. Innov.* 10, 91-101. DOI: 10.1016/j.eti.2018.02.003.

- Hoslett, J., Ghazal, H., Mohamad, N., and Jouhara, H. (2020). "Removal of methylene blue from aqueous solutions by biochar prepared from the pyrolysis of mixed municipal discarded material," *Sci. Total Environ.* 714, article 136832. DOI: 10.1016/j.scitotenv.2020.136832
- Ibrahim, T., Moctar, B. L., Tomkouani, K., Gbandi, D. B, Victor, D. K., and Phinthe, N. (2014). "Kinetic of the adsorption of anionic and cationic dye in aqueous solution by low-cost activated carbon prepared from sea cake and cotton cake," *American Chemical Science* 4(1), 38-57. DOI: 10.9734/ACSJ/2014/5403
- Jia, Z., Li, Z., Li, S., Li, Y., and Zhu, R. (2016). "Adsorption performance and mechanism of methylene blue on chemically activated carbon spheres derived from hydrothermally-prepared poly(vinyl alcohol) microspheres," *Journal of Molecular Liquids* 220, 56-62. DOI: 10.1016/j.molliq.2016.04.063
- Kuncoro, E. P., Isnadina, D. R. M., Darmokoesoemo, H., Dzembarahmatiny, F., and Septya, K. H. (2018). "Characterization and isotherm data for adsorption of Cd²⁺ from aqueous solution by adsorbent from mixture of bagasse-bentonite," *Data in Brief* 16, 354-360. DOI: 10.1016/j.dib.2017.11.060
- Liu, G., Liao, L., Dai, Z., Qi, Q., Wu, J., Ma, L. Q., Tang, C., and Xu, J. (2020). "Organic adsorbents modified with citric acid and Fe₃O₄ enhance the removal of Cd and Pb in contaminated solutions," *Chem. Eng. J.* 395, article 125108. DOI: 10.1016/j.cej.2020.125108
- Liu, G., Dai, Z., Liu, X., Dahlgren R. A., and Xu, J. (2022). "Modification of agricultural wastes to improve sorption capacities for pollutant removal from water A review," *Carbon Research.* 1, 24. DOI: 10.1007/s44246-022-00025-1
- Mallakpour, S., and Rashidimoghadam, S. (2019). "Poly (vinyl alcohol)/Vitamin C-multi walled carbon nanotubes composites and their applications for removal of methylene blue: Advanced comparison between linear and nonlinear forms of adsorption isotherms and kinetics models," *Polymer* 160, 115-125. DOI: 10.1016/j.polymer.2018.11.035
- Mashkoor, F., and Nasar, A. (2020). "Magnetized *Tectona grandis* sawdust as a novel adsorbent: Preparation, characterization, and utilization for the removal of methylene blue from aqueous solution," *Cellulose* 27, 2613-2635. DOI: 10.1007/s10570-019-02918-8
- Moorthy, A. K., Rathi, B. G., Shukla, S.P., Kumar, K., and Bharti, V. S. (2021). "Acute toxicity of textile dye Methylene blue on growth and metabolism of selected freshwater microalgae," *Environ. Toxicol. Pharmacol.* 82, article 103552, DOI: 10.1016/j.etap.2020.103552
- Muedi, K. L., Masindi, V., Maree, J. P., Haneklaus, N., and Brink, H. G. (2022). "Effective adsorption of Congo Red from aqueous solution using Fe/Al Di-metal nanostructured composite synthesized from Fe(III) and Al(III) recovered from real acid mine drainage," *Nanomaterials* 12, article 776. DOI: 10.3390/nano12050776
- Nakhjiri, M. T., Marandi, G. B., and Kurdtabar, M. (2018). "Poly (AA-co-VPA) hydrogel cross-linked with N-maleyl chitosan as dye adsorbent: Isotherms, kinetics and thermodynamic investigation," *Int. J. Biol. Macromol.* 117, 152-166. DOI: 10.1016/j.ijbiomac.2018.05.140
- Neolaka, Y. A. B., Lawa, Y., Naat, J., Lalang, A. C., Widyaningrum, B. A., Ngasu, G. F., Niga, K. A., Darmokoesoemo, H. Iqbal, M., and Kusuma, H. S. (2023). "Adsorption of methyl red from aqueous solution using Bali cow bones (*Bos javanicus domesticus*) hydrochar powder," *Results in Engineering* 17, article 100824. DOI:

- 10.1016/j.rineng.2022.100824
- Oladoye, P. O., Ajiboye, T. O., Omotola, E. O., and Oyewola, O. J. (2022). "Methylene blue dye: Toxicity and potential elimination technology from wastewater," *Results in Engineering*. 16, article 100678. DOI: 10.1016/j.rineng.2022.100678
- Ofudje, E.A., Williams, O. D., Asogwa, K. K., and Awotula, A. O. (2013). "Assessment of Langmuir, Freundlich and Rubunin Radushhkevich adsorption isotherms in the study of the biosorption of Mn (II) ions from aqueous solution by untreated and acid-treated corn shaft," *Int. J. Sci., and Eng. Res.* 4 (7), 1628-1634.
- Ofudje, E. A., Awotula, A. O., Alayande, O., Asogwa, K. K., and Olukanni, O. D. (2014). "Removal of lead (II) ions from aqueous solution by *Tricholoma terreum*: Kinetics studies," *Advances in Research* 2(2), 58-69. DOI: 10.9734/AIR/2014/7240
- Ofudje, E. A., Akinbile, B., Awotula, A. O., Oladipo, G. O., and Adedapo, E. A. (2015). "Kinetic studies of thiocyanate ions removal from aqueous solution using carbonaceous guinea-corn," *Journal of Science Research* 14, 94-101.
- Ofudje, E. A., Awotula, A. O., Hambate, G. V., Alayande, S. O., Ogundiran, A. A., and Olukanni, O. D. (2019). "Sorption of methylene blue by activated carbon primed from sugar cane bagasse," *Canadian Journal of Pure and Applied Sciences* 13(1), 4747-4764.
- Ofudje, E. A., Sodiya, E. F., Akinwunmi, F., Ogundiranc, A. A., Oladeji, O. B., and Osideko, O. A. (2022a). "Eggshell derived calcium oxide nanoparticles for Toluidine blue removal," *Desalination and Water Treatment* 247, 294-308. DOI: 10.5004/dwt.2022.28079
- Ouyang, X.-H., Wang, W.-Y., Yuan, Q.-P., Li, S.-X., Zhang, Q.-X., and Zhao, P.-X. (2015). "Improvement of lignin yield and purity from corncob in the presence of steam explosion and liquid hot pressured alcohol," *RSC Adv.* 5, 61650. DOI: 10.1039/C5RA12452B
- Paulo, H. F. P., Herman, C. J. V., Maria, O. H., Daniella, R. M., De Luz, S. M., and Da Silva, M. L. C. P. (2011). "Sugarcane bagasse pulping and bleaching: Thermal and chemical characterization," *BioResources* 6(3), 2471-2482. DOI: 10.15376/biores.6.3.2471-2482
- Pavan, F. A., Mazzocato, A. C., and Gushikem, Y. (2008). "Removal of methylene blue dye from aqueous solutions by adsorption using yellow passion fruit peel as adsorbent," *Bioresource Technol.* 99, 3162-3165. DOI: 10.1016/j.biortech.2007.05.067
- Peng, P., Jun-Li, R., Feng, X., Jing, B., Peng, P., and Run-Cang, S. (2009). "Comparative study of hemicelluloses obtained by graded ethanol precipitation from sugarcane bagasse," *J. Agric. Food Chem.* 57, 6305-6317. DOI: 10.1021/jf900986b
- Puchongkawarin, C., Jaiharn, W., Thongfuang, S., and Umpuch, C. (2020). "Comprehensive studies on methylene blue adsorption onto na-bentonite clay and its kinetics, isotherm and thermodynamics," *Materials Science and Engineering* 736, article 022013. DOI: 10.1088/1757-899X/736/2/022013
- Queen, A., Yusuf, M., Qadir, A., and Aamir, S. (2022). "Hospital wastewater treatment: Global scenario and case studies," DOI: 10.2166/9781789062625_0001
- Santhi, T., Manonmani, S., Smitha, T., and Mahalakshmi, K. (2009). "Adsorption of malachite green from aqueous solution onto a waste aqua cultural shell powders (prawn waste): Kinetic study," *Rasayan J. Chem.* 2(4), 813-824.

- Sewu, D. D., Boakye, P., and Woo, S. H. (2016). "Highly efficient adsorption of cationic dye by biochar produced with Korean cabbage waste," *Bioresource Technology*. DOI: 10.1016/j.biortech.2016.11.00
- Tasar, S. (2022). "Thermal conversion behavior of cellulose and hemicellulose fractions isolated from tea leaf brewing waste: Kinetic and thermodynamic evaluation," *Biomass Conv. Bioref.* 12, 2935-2947. DOI: 10.1007/s13399-021-01697-2
- Turgay, T., Murat, E., Burak, C., and Selhan, K. (2012). "Adsorption of methylene blue from aqueous solution on activated carbon produced from soybean oil cake by KOH activation," *BioResources* 7(3), 3175-3187. DOI: 10.15376/biores.7.3.3175-3187
- Uzosike, A. O., Ofudje, E. A., Akiode, O. K., Ikenna, C. V., Adeogun, A. I., Akinyele, J. O., and Idowu, M. A. (2022). "Magnetic supported activated carbon obtained from walnut shells for bisphenol-a uptake from aqueous solution," *Applied Water Science* 12, 201 DOI: 10.1007/s13201-022-01724-1.
- Wang, J., Tan, Y., Yang, H., Zhan, L., Sun, G., and Luo, L. (2023). "On the adsorption characteristics and mechanism of methylene blue by ball mill modified biochar," *Sci. Rep.* 13, article 21174. DOI: 10.1038/s41598-023-48373-1
- Wu, K.-L., Pan, X.-M., Zhang, J.-Q., Zhang, X.-M., Salah zene, A., and Tian, Y.-Q. (2020). "Biosorption of Congo Red from aqueous solutions based on self-immobilized mycelial pellets: Kinetics, isotherms, and thermodynamic studies," ACS Omega 5, 24601-24612. DOI: 10.1021/acsomega.0c03114
- Xia, Y.-X., Yao, Q., Zhang, W., Zhang, Y.-S., and Zhao, M.-J. (2015). "Comparative adsorption of methylene blue by magnetic baker's yeast and EDTAD-modified magnetic baker's yeast: Equilibrium and kinetic study," *Arabian Journal of Chemistry* 12(8), 2448-2456. DOI: 10.1016/j.arabjc.2015.03.010
- Yashni, G., Al-Gheethi, A., Marlinda, A. M., Mawar, M. A., Al-Sahari, M., Radin, M. S. R. M., Sadeq, A., and Efaq, N. (2020). "Removal of Basic Brown 16 from aqueous solution using durian shell adsorbent. Optimisation and techno-economic analysis," *Sustainability* 12, article 8928. DOI: 10.3390/su12218928
- Yavuz, O., and Saka, C. (2013). "Surface modification with cold plasma application on kaolin and its effects on the adsorption of methylene blue," *Applied Clay Science* 85, 96-102. DOI: 10.1016/j.clay.2013.09.011
- Zha, Q., Sang, X. Liu, D., Wang, D., Shi, G., and Ni, C. (2019). "Modification of hydrophilic amine-functionalized metalorganic frameworks to hydrophobic for dye adsorption," *Journal of Solid State Chemistry* 275, 23-29. DOI: 10.1016/j.jssc.2019.04.001

Article submitted: September 9, 2024; Peer review completed: September 28, 2024; Revised version received: September 30, 2024; Accepted: October 3, 2024; Published: October 16, 2024.

DOI: 10.15376/biores.19.4.9191-9219